The Journal of the Oceanological Society of Korea
Vol. 22, No. 4, p.217-227, December 1987.

A Study on the Heat Budget in the South Eastern Area of the Yellow Sea

Hyun Chul Lee and Hui Soo An
Seoul National University, Seoul 151, Korea

황해 남동해역에서의 열수지에 관한 연구

이현철 · 안희수
서울대학교 사범대학 지구과학교육과

Abstract

The heat budget of the south eastern region (33°N-36°N, 120°E-125°E) of the Yellow Sea was calculated by using the meteorological and oceanographical data. The sensible heat, the evaporation heat and the long wave back radiation have annual variation and increases toward south with strong gradient along the Cheju channel in winter, but they all show tendency to decrease toward eastern coastal area in summer. The area is roughly divided into three parts, the central part, the coastal part and the southern part, according to the characteristics of variation and distribution patterns of the exchanged heats. The amplitude of the annual variation of total heat exchange in the southern part is very large compare to those of the central and coastal part. The studied area is appeared to be heated mainly by the evaporation heat and the sensible heat, based on the results of this study.

요약 : 황해동남해역 (33°N-36°N, 120°E-125°E) 의 해면 열수지를 기상자료와 해양자료를 이용하여 계산하였다. 현열, 증발열, 장파복사열은 모두 년변화를 하고 겨울철에는 제주 해협을 따라 강한 온도 전선을 나타내지만 여름철에는 동쪽 연안해역을 향해 감소하는 경향을 가진다. 전해역은 교환열량의 년변화 및 분포의 특징에 따라 중앙해역, 연안해역, 남부해역으로 나뉘어진다. 남부해역의 총교환열량의 년변화 진폭은 중앙해역, 연안해역에 비하여 매우 크다. 대체적으로 조사해역은 증발열과 현열에 의해 가열된다고 볼 수 있다.

INTRODUCTION

The oceanic condition of the Yellow Sea is strongly affected by the monsoon. Under the influence of the dry and cold continental air mass in winter and the warm maritime tropical air mass in summer, the annual range of sea surface temperature variation of the area is over 20℃. The heat exchange through the sea surface mainly determines the vertical and horizontal temperature distribution. Especially the evaporation heat and the sensible heat are important boundary condition for the meteorological study (Manabe, *et al.*, 1975).

Jacobs(1942) estimated the heat budget of the Pacific Ocean and the Atlantic Ocean using the empirical relationships. In the numerical study of the idealized baroclinic ocean(Haney, 1971, 1974), the lateral heat transport and the downward flux over the ocean were calculated by using the relationship of the heat balance. The exchanged heat flux in the North Pacific Ocean was

estimated by the bulk-aerodynamics (Bunker, 1976). The satelite data were used for the calculation of the albedo, the infrared flux and the absorption ratio over the global scale(Stephan, *et al.*, 1981). In the previous research Han(1970) calculated the evaporation heat and the sensible heat in this area during January in 1968 and in 1969.

DATA ANALYSIS AND TEMPERATURE DISTRIBUTION IN THE STUDY AREA

Data and data analysis

The data collected by the Fisheries Research and Development Agency of Korea for fifteen years(1961−1975) in the every even month are used for the analysis of heat budget. Fig. 1 represents the observation points in the studied area. Since the scale of oceanic phenomena is one order smaller than those of the meteorological ones, the meteorological data of Mogpo station are assumed to be represented the meteorological parameters of the area except the wind velocity. Air temperature, air pressure and cloudness data are collected from the Monthly Weather Report published by the Central Meteorological Office of Korea for ten years(1961−1970). The wind velocity data are collected from the results of marine meteorological and oceanographical observations made by Japan Meteorological Agency for fifteen years(1961−1975) over the region that involves the studied area, 33°N-36°N, 120°E-125°E(Kutsuwada, 1982). The original data were smoothed out by using Fourier method. The first three Fourier coefficients of meteorological data are taken from the harmonic analysis. Fig. 2 shows the results of the harmonic analysis.

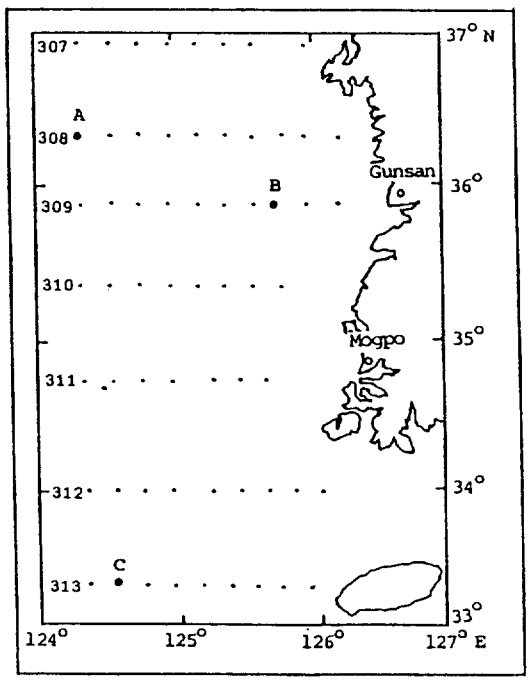

Fig. 1. The observation points in the studied area. (A : 308−10, B : 309−3, C : 313−6)

Horizontal temperature distribution in the area

Under the influence of the monsoon, the sea temperature in the area has the distinctive feature in winter and in summer respectively. Fig. 3 represents the horizontal temperature distribution at surface and at 50 *m* depth over the area in February.

For the convenience of study, the area is divided by the horizontal temperature distribution into three parts, the central part (station A, 308−10), the coastal part(station B, 309−3) and the southern part of the Yellow sea(station C, 313−6), as shown in Fig. 1. The temperature of southern part is higher than that of the northern part and the central part is warmer than the coastal part. The temperature distribution at surface and 50 m depth are almost similar. Fig. 4 shows the horizonlal temperature distribution at surface and 50 *m* depth over the area in August. There is no Temperature difference between the central part and the southern part.

The surface temperature ranges from

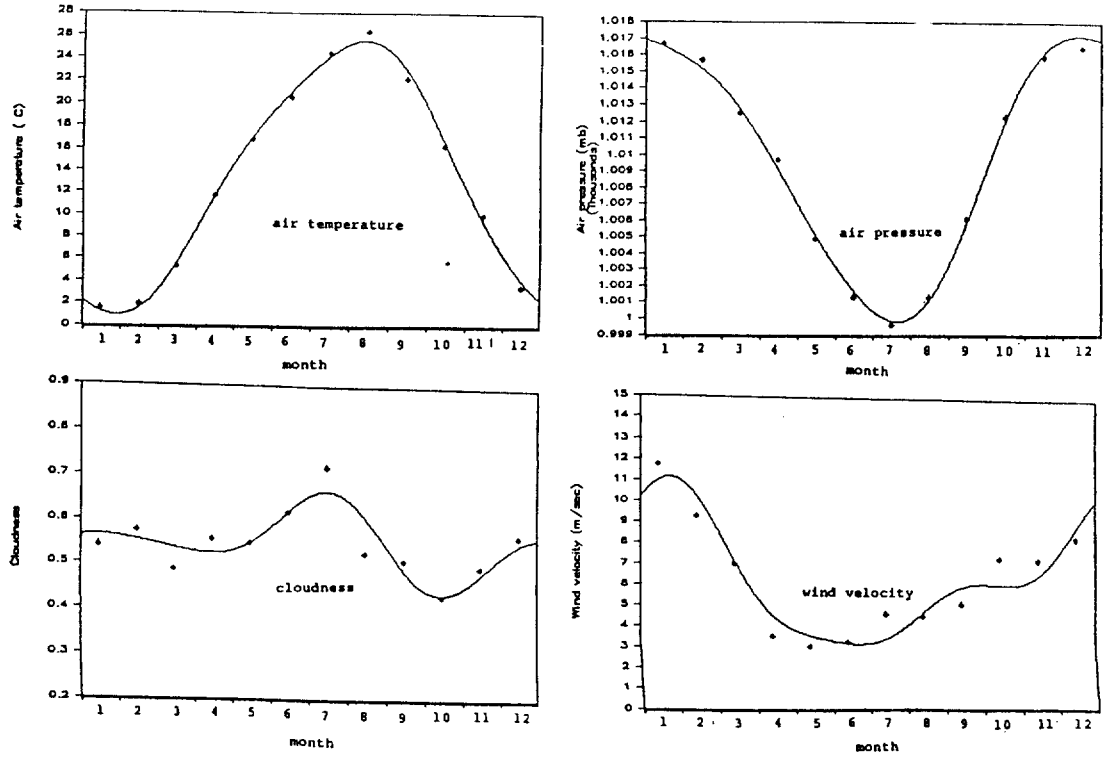

Fig. 2. The annual variation of meteorological data. (solid line ; calculated, dark points ; real data)

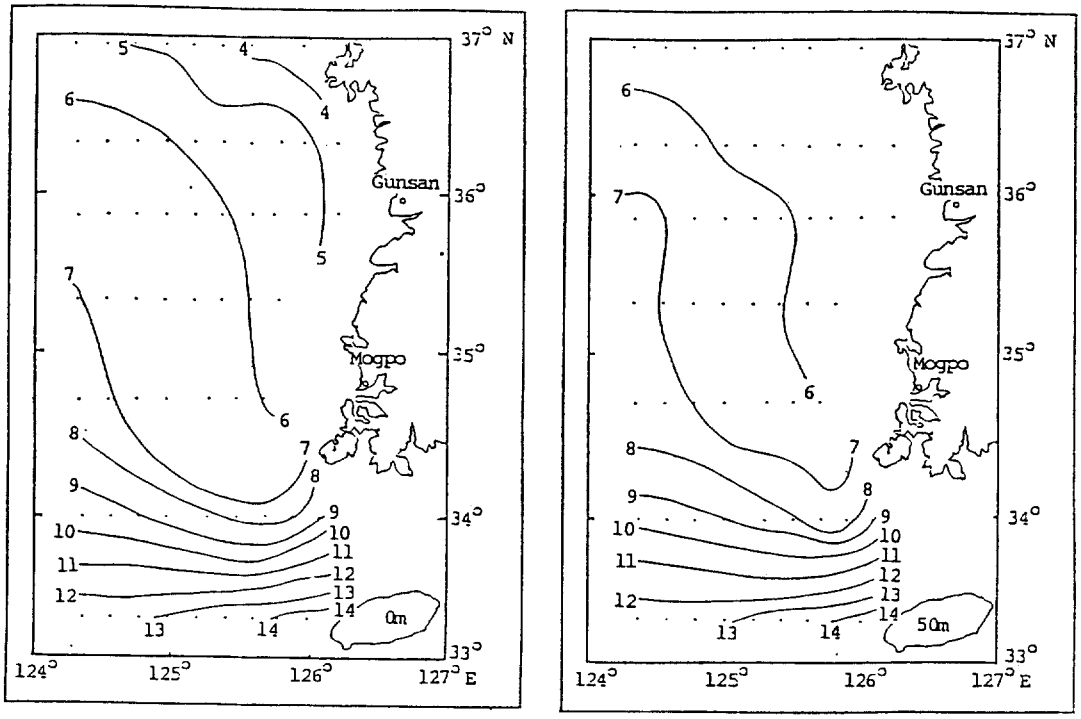

Fig. 3. Horizontal temperature distribution in February at surface (left) and 50 meters (right) (℃).

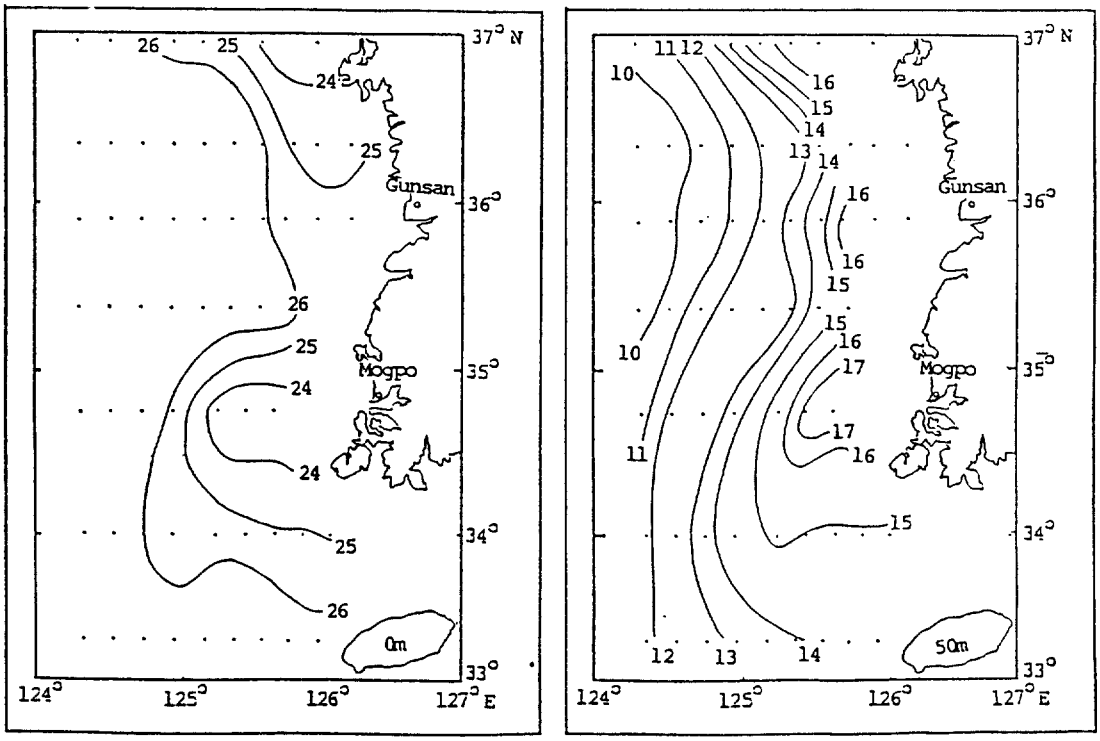

Fig. 4. Horizontal temperature distribution in August at surface(left) and 50 meters(right) (℃)

24℃ to 26℃ and this is about 10℃ higher than that of the 50 m depth. However, the temperature gradient from center to coast is definitely reversed.

At surface, the central part is warmer than the coastal part and vise versa at 50 m depth. The temperature difference between surface and 50 *m* depth are quite large in the central part compare to the coastal part and this should be attributed to vertical mixing by the tidal motion in the coast (An, 1986).

The sea surface temperature Ts, the air temperature Ta and the sea-air temperature difference Ts-Ta at the three stations (A, B, C) representing the three parts are shown in Fig. 5. For all the three stations, the sea surface temperature has the maximum value in August and the difference of sea-air temperature has maximum value in January or February and minimum value in May.

FORMULATION OF HEAT BUDGET

The basic assumption for this formulation is that the ocean is in contact with the atmosphere in equilibrium state of heat flow. The heat budget equation is as follows

$$Qs-(Qb+Qe+Qh)=Qv+Qt$$

where Qs is the net solar radiation, Qb the effective long wave radiation of sea surface, Qh the sensible heat, Qe the evaporation heat, Qv the advective heat by current and Qt is the heat storage in the ocean. Because there has been no observation of the strong currents in the area of the Yellow Sea (Lie, 1984), we neglect the advective heat Qv in this study.

The downward flux of solar radiation which penetrates the ocean surface, Qs, can be calculated by the following equation (Gill,

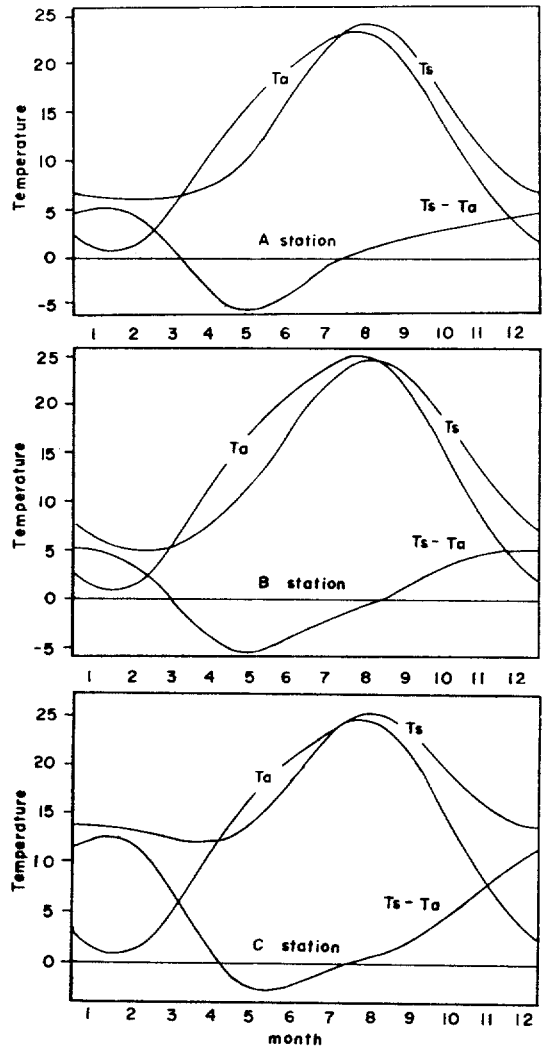

Fig. 5. The annual variation of sea surface temperature(Ts), air temperature(Ta) and the difference between Ts and Ta at station A, B and C(℃).

1982).

$$Qs(t) = Qso(t) \cdot (1-\alpha_s) \cdot \{1-0.7\,Nc(t)\}$$

where Qso is the incident flux at the top of cloud and cloudness Nc, and the albedo of sea surface, α_s.

Kang(1984) used the following equation for the calculation of Qso.

$$Qso(t) = 354+180\cos(\omega t-173)\{Watt/m^2\}$$

where ω is the angular velocity with the value of 360°/365 day. The albedo of sea surface is 0.06 and the cloudness Nc is given by the harmonic analysis as follows.

$$\begin{aligned} Nc(t) = {} & 0.574+0.05\cos(\omega t-152.89) \\ & +0.068\cos(2\,\omega t-29.51) \\ & +0.018(3\,\omega t-266.62) \end{aligned}$$

The net long wave radiation, Qb, is given by the following relationship (Kraus and Rooth, 1961).

$$\begin{aligned} Qb(t) = {} & 0.985\,\sigma Ts^4(t)\{0.39-0.05(e_a(t))^{1/2}\} \\ & \times(1-0.6\,Nc^2) \end{aligned}$$

where σ is the Stephan-Boltzmann constant, Ts is the sea surface temperature(° K), and e_a the vapor pressure(mb) above the sea level, which is given by the Clausius -Clapeyron equation

$$e_a(t) = \gamma \times 10\,EXP\{9.4051-2353/Ta(t)\}$$

where γ is the relative humidity, 0.75, from the annual mean for 1951-1980(Lie, 1984).

The upward heat flux of the sensible and latent heat are parameterized by the turbulent transfer formulas. The sensible heat flux formula is given by Wyrtki(1965) as follows.

$$Qh(t) = \rho_a \times Ch \times Cp \times \omega(t)\{Ts(t)-Ta(t)\}$$

where ρ_a is the mean air density, 1.2×10^{-3} (g/cm^3), Cp is the specific heat of air, 0.24(cal/g℃), Ts and Ta are sea surface and air temperature respectively. Ch is the drag coefficient or Dalton number, which is 0.83×10^{-3} at stable state and 1.10×10^{-3} at unstable state of boundary layer. In this paper, the stable state is that the air is warmer than the sea and vice versa. The formulation of the evaporation heat(Qe) is given as follows(Haney, 1971).

$$Qe(t) = a \times Cd \times \omega(t) \cdot L \cdot \{qs(t)-qa(t)\}$$

where L is the latent heat of evaporation, Cd the drag coefficient or the Stanton number 1.5×10^{-3}(Gill, 1982), qs(t) and qa(t)

are the saturation specific humidity of the sea surface and air respectively. The data of the wind velocity is smoothed out by harmonic analysis as follows.

$$W(t) = 6.26 + 3.24\cos(\omega t - 6.28) + 1.30\cos(2\omega t - 7171) + 0.63\cos(3\omega t - 148.74), \text{(m/sec)}$$

THE RESULTS OF THE ANALYSIS

The horizontal distribution of the exchanged heats

With the sea surface temperature and the data of meteorological observation, the horizontal distribution of the effective back radiation, the sensible heat, the evaporation heat, and downward storage heat are estimated by the heat budget model over the area (61 points in Fig. 1).

The effective back radiation Qb : Fig. 6 shows the horizontal distribution of the monthly effective back radiation Qb over the area. In winter season, because of the high sea temperature in the southern area and the low temperature in northern area, the large gradients of the effective back radiation(170 ly/day to 178 ly/day) is appeared between 34°N and 33.20°N. In

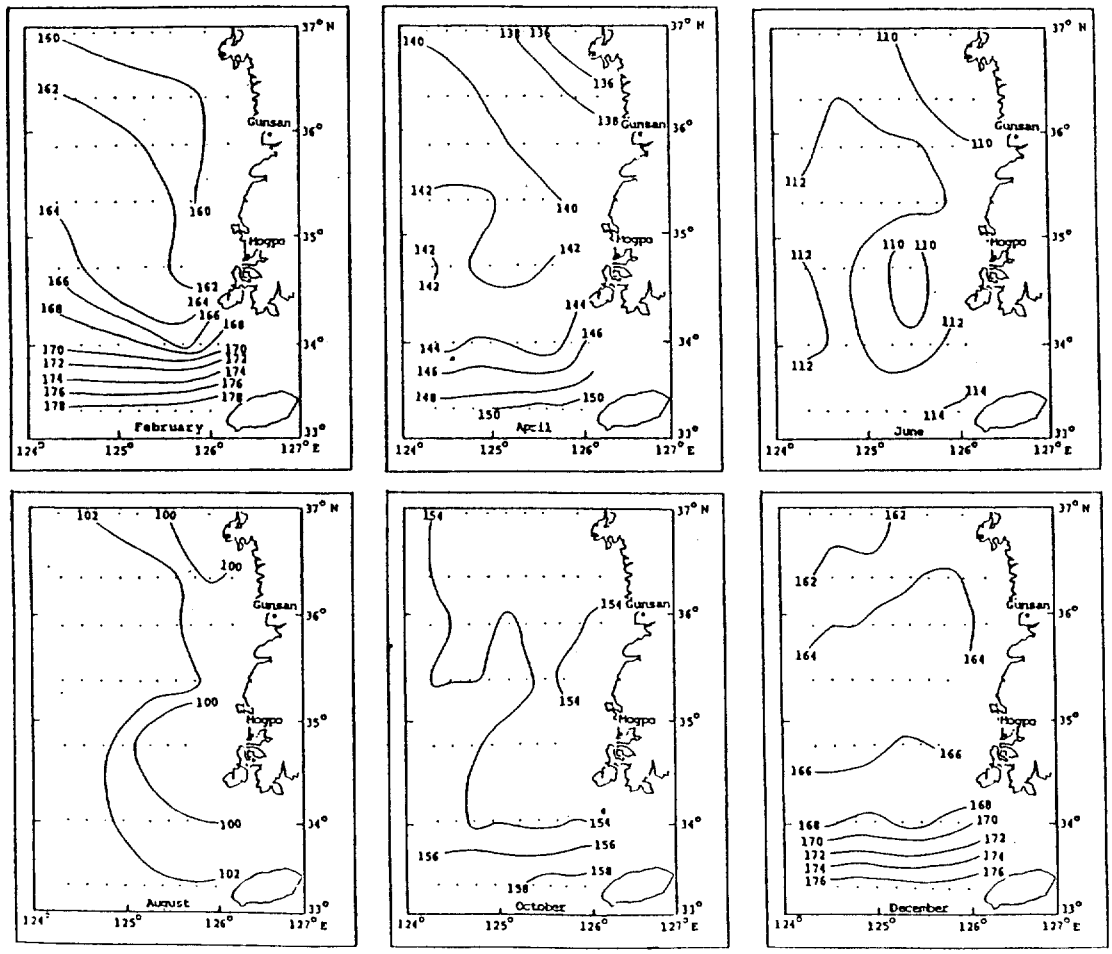

Fig. 6. The horizontal distribution of effective back radiation Qb(ly/day).

June and August, the amount is less than 110 ly/day because the high cloudness(from Fig. 2) reduces the back radiation from the sea in spite of the high sea surface temperature.

The effective back radiation varies only between 100 ly/day and 102 ly/day in August and the strong gradient along the 34°N line disappears in summer season. But in December and February, it is quite high (>160 ly/day) because of the low cloudness and the high vapor pressure. The variation of the effective back radiation is chiefly affected by the cloudness and the vapor pressure.

The Sensible heat Qh : The distribution of the sensible heat(Fig. 7) is determined by the difference between temperature of sea surface and air temperatures. The pattern of distribution is quite different between summer and winter. In December and February, the difference of the sensible heat between the southern part(300 ly/day) and the central part(<200 ly/day) is quite large and all values are positive (heat loss).

From April, the value of sensible heat of the central regions turns negative (the incoming sensible heat). The negative turning is started from the north and the whole area changes negative in June because the sea

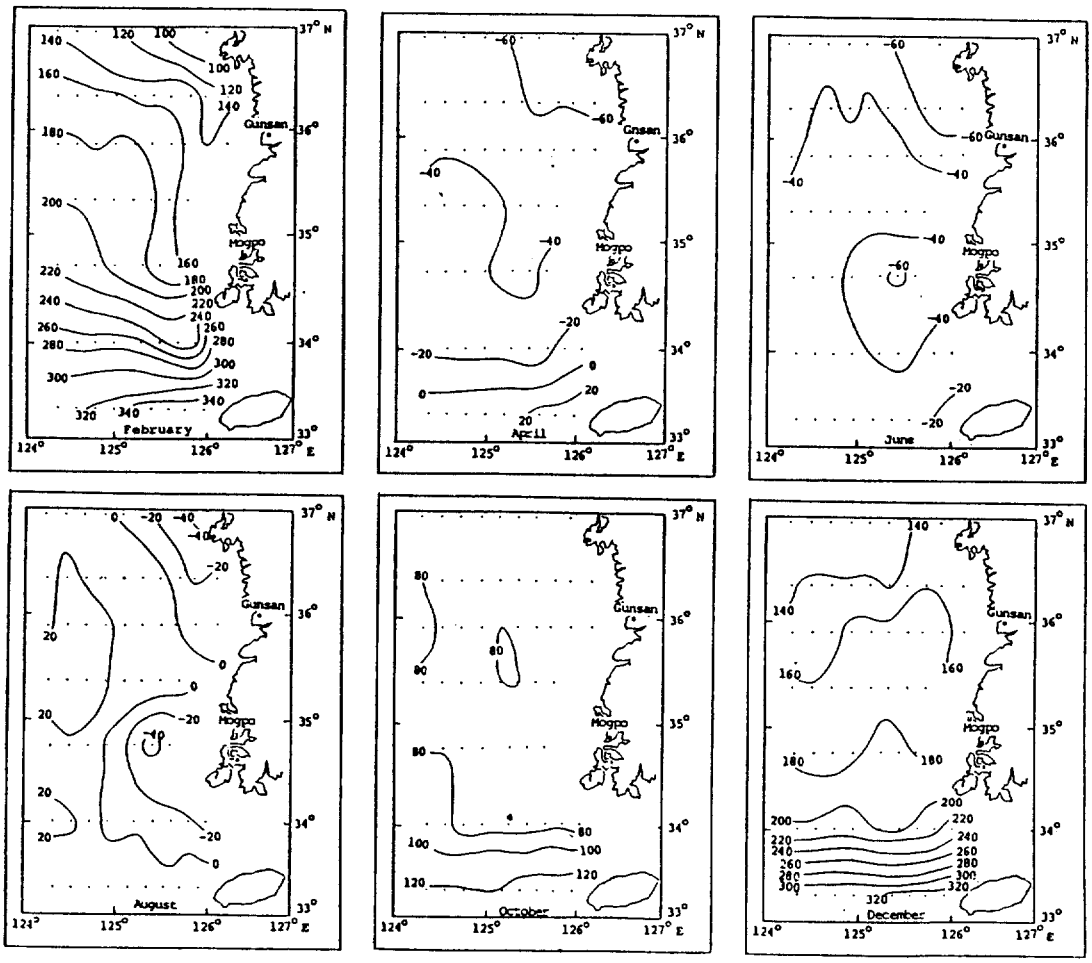

Fig. 7. The horizontal distribution of sensible heat Qh(ly/day).

surface of the coastal part is cooler than that of the central part in August. In December and February, the sensible heat values are all positive(140 ly/day to 300 ly/day) due to the large difference between sea and air temperature. The southern part losses the largest sensible heat(>260 ly/day) because of the high sea surface temperature that is due to the effect of Kuroshio Currents. Han(1970) calculated the average sensible heat loss of 225 ly/day in 1968 and 233 ly/day in 1969 during January.

The evaporation heat Qe : The distribution of the heat used for evaporation(Fig. 8) is determined by the vapor pressure difference between air and sea surface and wind velocity. The distribution of the evaporation heat is also significantly different between in winter and in summer. Roughly speaking, it is large in winter and small in summer. Many contour lines crowd along the latitude of Cheju channel in winter. This distribution distinguishes the central part(140 ly/day to 200 ly/day) from the southern parts(>300 ly/day). The lowest evaporation occurs in June due to the small vapor pressure difference between air and sea surface when it is used to be less than 20 ly/day. In August, many contour lines made a front between the coastal part and the central part because the low temperature induces the low

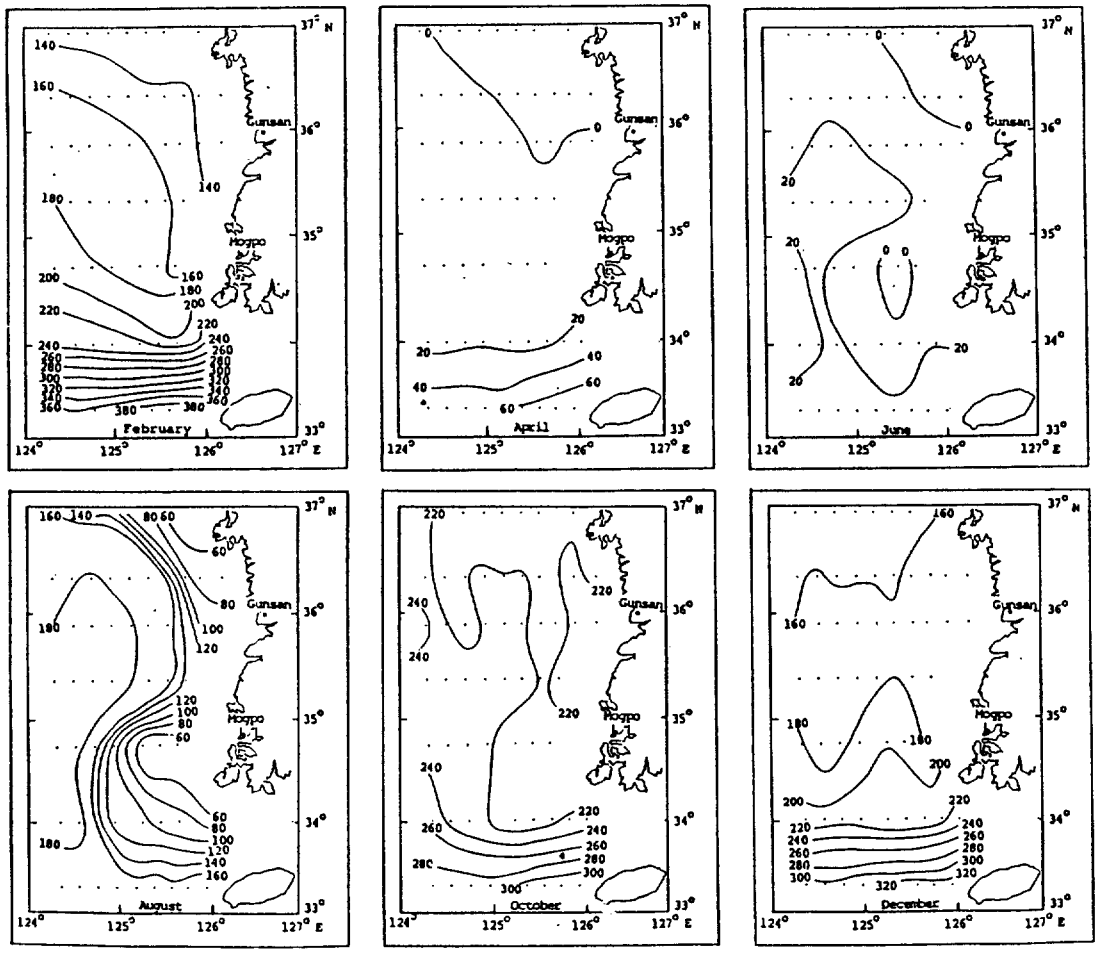

Fig. 8. The horizontal distribution of evaporation heat Qe(ly/day).

vapor pressure difference between air and sea surface.

Han(1970) estimated the average heat losses of evaporations of 264 ly/day and 220 ly/day in the northern part in January, 1968 and 1969 respectively. And the average annual amount of the heat used for evaporation over the southern part was calculated less than 300 ly/day by Wyrtki(1965).

The distribution of the total heat exchange Qt : The total heat exchange across the sea surface is shown in Fig. 9. In February, the total heat exchange in the southern part (< −500 ly/day) is more than five times of that in the central part. The total heat loss in the southern part is very high, due to the effect of the Kuroshio current, especially in winter. From April to August the whole area gains heats across the sea surface and the maximum appears in June. In summer, the received heat along the coastal part(> 300 ly/day), where the active tidal mixing processes occur, is larger than that in the central part(200 ly/day to 250 ly/day). The average annual heat loss in the southern regions of 34°N is about-180 ly/day and the average annual heat gain in the northern regions on 34°N is more than 500 ly/day. This means that the southern region on 34°N

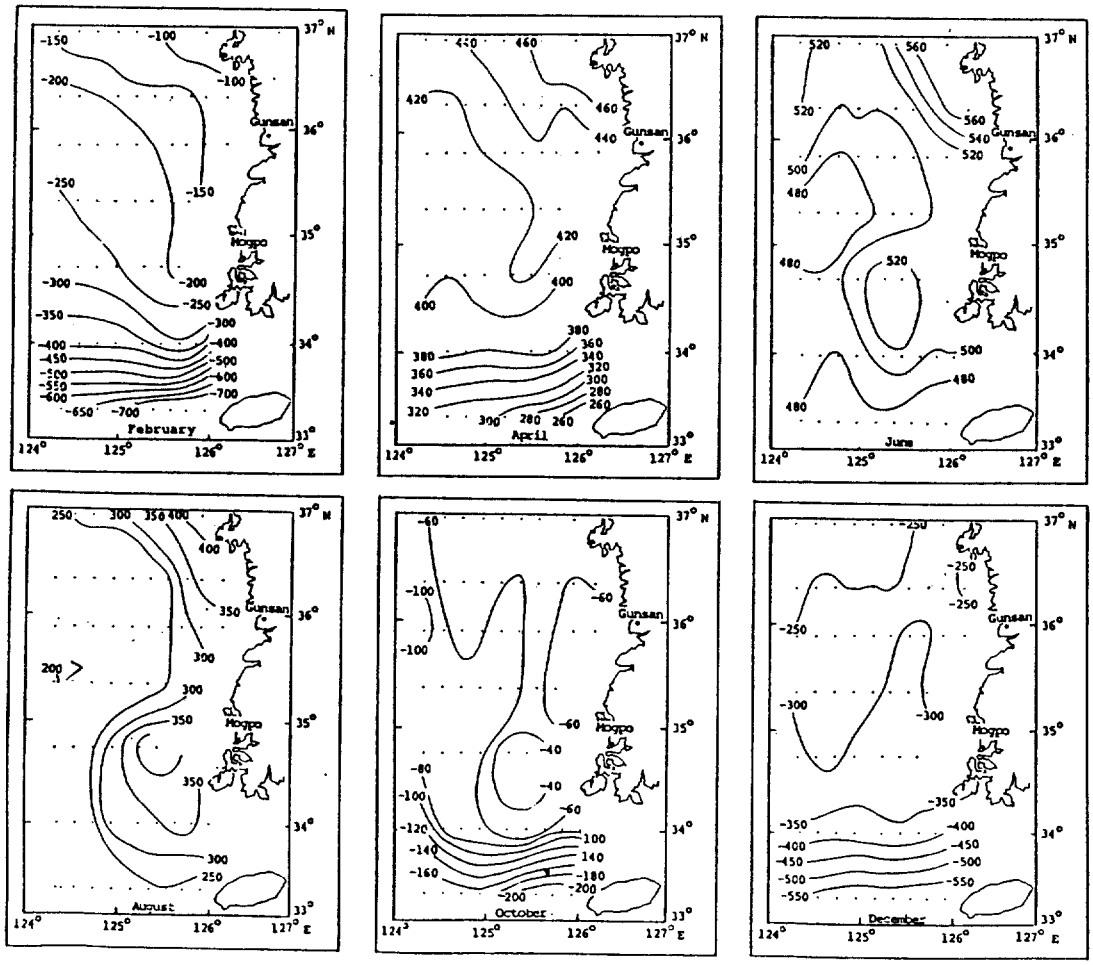

Fig. 9. The horizontal distribution of total heat exchange Qt(ly/day).

which is included in the Kuroshio region is a sink of heat in the North Pacific subtropical ocean circulation(Wyrtki, 1965) and in the northern regions of 34°N the vertically homogeneous cold water is appeared due to the strong north westerly wind in winter season.

The annual variation of the exchanged heat

The exchanged heats through the surface were calculated from the empirical equations as stated above. The annual variations of Qs, Qb, Qe, Qh and Qt at the central part(station A), the coastal part(station B), and the southern part(station C) of the Yellow Sea are shown in Fig. 10.

The solar radiation Qs shows the same features all over the area which has the minimum value in December and the maximum in May. The effective back radiation Qb has very small amplitude compare to the others and minimum value in July.

The annual variation of the evaporation heat Qe has two peaks in January and in September, and has the minimum value in May and in December in all area. Since the temperature of sea surface is warmer than that of the air in January, the air-sea vapor pressure is increased. This effects lead to the peak in January. In the same manner, the increase of wind velocity and the air-sea vapor pressure difference lead to another peak in Septmeber.

The peak values of Qe in September at stations A and B are the higher than those in January. But at station C, the January peak of Qe (500 ly/day) is greater than the September one (354 ly/day).

The sensible heat Qh has the negative value at the three stations, (A, B, C) from April to July. In this period the sea is heated by the sensible heat. The sensible heat is directly affected by the sea-air temperature difference and the stability of the atmospheric surface layer. The striking feature of the sensible heat variation is that the maximum value of the southern part(420 ly/day) appears in January.

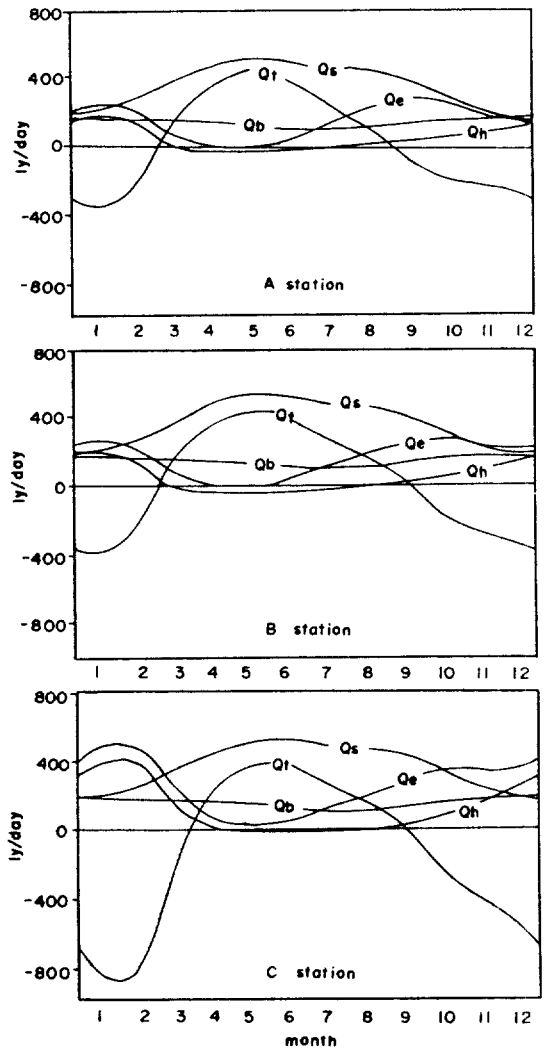

Fig. 10. The annual variation of Qs, Qb, Qe, Qh and Qt at station A, B and (ly/day).

The total heat exchange Qt represents the differences between downward and upward heats through the surface. The sea waters are heated during the summer when the value of Qt is positive, and they are cooled during the winter inversely. At station A, the minimum value of Qt is -362

ly/day in January, and the maximum value is 530 ly/day in May. The variations of the station B are similar to those of the station A, the minimum and the maximum values of the station B are −400 ly/day in January and 420 ly/day in May respectively. The sea surface at the station C keeps up the high temperature during the winter time, owing to the effect of the Kuroshio Current. The minimum value of Qt in January is −870 ly/day that is ten times of the emitted heat flux at the station A and the station B.

CONCLUSION

The effective back radiation, the sensible heat, the evaporation heat and the total heat exchange in the area change in time and in place. They all show annual variation. The sensible heat is maximum in winter and minimum through spring and summer and the effective back radiation is maximum in winter and minimum in summer. But the evaporation heat diagram shows two maximum in January and in September. Based on the characteristics of variation and distribution of the exchanged heats. The area is divided into three parts ; the central part, the coastal part and the southern part, the amplitude of the annual variation in the southern part is very large compare to those of the central and coastal parts.

As a result, it can be said that the ocean is heated chiefly by the evaporation heat and the sensible heat.

ACKNOWLEDGEMENTS

This research was supported by the Ministry of Education of Korea.

REFERENCES

An, H. S., 1987. Dynamical mechanism for the fronts around the Yellow Sea Cold Water Mass. J. Korean Earth Science Society, 7(2) : 101~107.

Bunker, A.F., 1976. Computations of surface energy flux and annual air-sea interaction cycles of the North Atlantic Ocean. Monthly Weather Review, 104 : 1122~1140.

Central Meteorological Office of Korea, 1961~1970. Monthly weather reports.

Fisheries Research and Development Agency of Korea, 1961~1975. Annual reports of oceanographic observations.

Gill, A.E., 1982. Atmosphere-ocean dynamics, Academic Press, 30 p.

Han, Y.H., 1970. On the estimation of evaporation and sensible heat transfer in the part of the Yellow Sea in the month of January. Korean Met. Soc. 6(2) : 83~87.

Haney, R, 1., 1971, Surface thermal boundary condition for ocean circulation model, J. Phys. Oceanogr., 1(4) : 241~248.

———, 1974. A numerical study of the response of an idealized ocean to large scale heat and momentum flux, J. Phs. Oceanogr., 4 : 145~167.

Jacobs, W.C., 1942. On the energy exchange between sea and atmosphere. J. Marine Research, 1 : 37~66.

Japan Meteorological Agency, 1961~1975. Results of marine meteorological and oceanographical observations.

Kang, Y.Q., 1984. Atmospheric and oceanic factors affecting the air-sea thermal interactions in the East Sea (Japan Sea). J. Oceanol. Society of Korea, 19(2) : 163~171.

Kraus, E.B., and C. Rooth, 1961. Temperature and steady state vertical heat flux in the ocean surface layers. Tellus, 13 : 231~238.

Kutsuwada, K., 1982. Climatological maps of wind stress field over the North Pacific Ocean. The Oceanographical Magazine, 32(1~2) : 25~46.

Lie, H.J., 1984. A note on water masses and general circulation in the Yellow Sea(Hwanghae). J. Oceanol. Society of Korea, 19(2) : 187~194.

Manabe, S., K. Bryan and M. J. Spelman, 1975 A global ocean-atmospheric climatic model : Part I. The atmospheric circulation. J. Phys. Oceanogr., 5(1) : 3~46.

Stephan, G.L., G.G. Compbell and T.H.V. Haar, 1981. Earth radiation budgets. J. Geophys. Res., 86 C(10) : 9739~9760.

Wyrtki, K., 1965. The average annual heat balance of the North Pacific Ocean and its relation to ocean circulation. J. Geophys. Res., 70(18) : 4547~4559.

Received July 15, 1987
Accepted December 4, 1987